Effect Of Welding Process on Microstructure and Pitting Corrosion Behavior of AA2014 Al-Cu Alloy Welds

V. S. N. Venkata Ramana[1], K. Ratna Kumar[2], G. Madhusudhan Reddy[3] and K. Srinivasa Rao[4]
[1] Department of Mechanical Engineering, GITAM Institute of Technology, GITAM University, Visakhapatnam - 530045. India.
[2] Department of Metallurgical Engineering, Government Polytechnic, Visakhapatnam - 530 007. India. [3] Metal Joining Group, Defence Metallurgical Research Laboratory, Hyderabad - 500 058. India. [4] Department of Metallurgical Engineering, Andhra University College of Engineering (A), Visakhapatnam- 530 003. India. Email: arunaraok@yahoo.com

ABSTRACT

Wrought AA 2014 Al-Cu alloy in mill annealed (O) condition and naturally aged (T4) condition was welded by the Gas Tungsten Arc Welding (GTAW) and Friction Stir Welding (FSW) processes. The microstructural changes and pitting corrosion behaviour in all zones of welds for both the welding processes have been investigated when the alloy was welded in O as well as in T4 conditions. It was observed that naturally aged (T4) alloy weld exhibited better corrosion properties than annealed (O) alloy weld this is attributed to the precipitation of fine grained eutectics in T4 alloy during welding. The pitting corrosion resistance was found to be better and uniform through out cross section of the friction stir welds compared to GTA welds, indicating improvement in corrosion properties of the welds in solid state welding.

Keywords: Gas Tungsten Arc Welding, Friction Stir Welding, AA2014 alloy, Partially Melted Zone, Thermo-mechanically Affected Zone, Pitting Corrosion, Potentiodynamic Polarization.

1.0   INTRODUCTION

Addition of alloying elements like copper, magnesium and silicon significantly contribute to strength of aluminum alloys by precipitation hardening. Due to the limited solubility of these elements in aluminium, these alloying elements are often distributed not only in the aluminum solid solution, but also in fine precipitates and coarse intermetallic particles. These particles, viz., $CuAl_2$ and Mg_2Si play a crucial role in the welding of heat treatable aluminum alloys which mainly induce liquation in the partially melted zone (PMZ). The heat treatable aluminum alloys are known to be susceptible to cracking in the PMZ area of the weld. Huang and Kou [1-3] recently studied PMZ liquation in the gas metal arc welds of alloys AA2219, AA2014, AA6061 & AA7075 including the liquation mechanization and found that significant weakening of PMZ is caused by grain boundary segregation. Even though the preferred welding method for aluminum alloys is alternating current GTA welding process, several investigators have identified a number of advantages and disadvantages of the pulsed current technique [4-7].

Keeping in view the problems of fusion welding of medium strength aluminum alloy AA2014, friction stir welding processes was used. In the present work, it is aimed to investigate the microstructural changes and pitting corrosion behavior when AA2014 alloy is welded in GTA and friction stir welding processes and compare the two in the light of better corrosion properties and microstructural features.

Friction stir welding process was based on friction heating at the faying surfaces of two pieces to be joined, results in a joint created by interface deformation, heat and solid-state

29

diffusion [8]. It is essentially a hot-working process where a large amount of deformation is induced into the work piece through pin and shoulder and the temperature never exceeds 0.8 Tm [9]. It results in a distinguished microstructure in precipitation hardenable aluminum alloys [10-12]. The first attempt at classifying micro-structures was made by P. L. Threadgill, [13]. This was further revised and accepted by the friction stir welding licenses association. This system divides the weld zone into unaffected material or parent metal (PM), heat affected zone (HAZ), thermo-mechanically affected zone (TMAZ) and weld nugget zone (NZ).

2.0   EXPERIMENTAL PROCEDURE

The parent metal employed in this work is wrought AA2014 alloy [4mm thick plates] in mill annealed (O) and T4 (Solution heat treated at 540^{0}C for 1 h and aged at room temperature for 30 days) conditions. The composition of the alloy is given in **Table 1**. Gas Tungsten Arc and Friction Stir welding processes have been used in the present investigation. Specially designed tool made of tool steel has frustum shaped probe (7 mm diameter & 3.5 mm height) with threads and shoulder diameter 15 mm is used in this study. Details of the welding parameters used are given in **Table 2** and **Table 3**.

Table 1: Chemical composition of base metal AA 2014 and filler material AA4043

Element	AA2014	AA4043
Cu	4.5	0.25
Mg	0.4	0.05
Si	0.8	5.20
Fe	0.7	0.8
Mn	0.8	0.05
Al	Balance	Balance

Prior to welding, the base material coupons and filler wire were brushed and thoroughly cleaned with acetone. The welded samples were sectioned and mounted in bakelite. After mechanical polishing using 120 to 600 grit SiC papers, the samples were polished using alumina powder on rotating wheels. Etching was done using Keller's reagent. The microstructures were recorded with Image analyzer attached to the optical microscope and also using scanning electron

Table 2: Welding parameters used in continuous current GTA welding

Welding parameter	Value
Current	385A
Voltage	7.2V
Welding speed	200mm/min
Shielding gas	Argon
Gas flow rate	16 l/min
Filler feed rate	2200 mm/min

Table 3: Welding parameters used in friction stir welding

Welding parameter	Value
Load	10.0 KN
Speed of rotation	800 rpm
Speed of welding	135 mm/min.

microscope (SEM). Potentiodynamic polarization tests were carried out to determine the pitting potential. Vickers hardness testing was carried out on weld, TMAZ and HAZ+ regions of the samples with 5 kg load and 15 seconds dwelling time.

3.0   RESULTS AND DISCUSSION

3.1   Microstructure studies

3.1.1 Base Metal

Formation of intermetallic phases and precipitates depend mainly on the chemical composition of aluminium alloy. The prior condition of the alloy affects size and distribution of these phases. Optical micrographs of the base metal AA2014 in O and T4 conditions are shown in **Fig. 1**. The microstructures consisted of white matrix of α-solid solution grains and second phase particles appearing black in color. Microstructures of the base metals clearly reveal that relatively fine and uniformly distributed eutectics are present in T4 condition, where as coarse and non-uniformly distributed eutectics in O condition. SEM micrographs of base metal AA2014 in O and T4 conditions are shown in **Fig. 2**. Large particles (2-10 μm) were present both within grains and at grain boundaries.
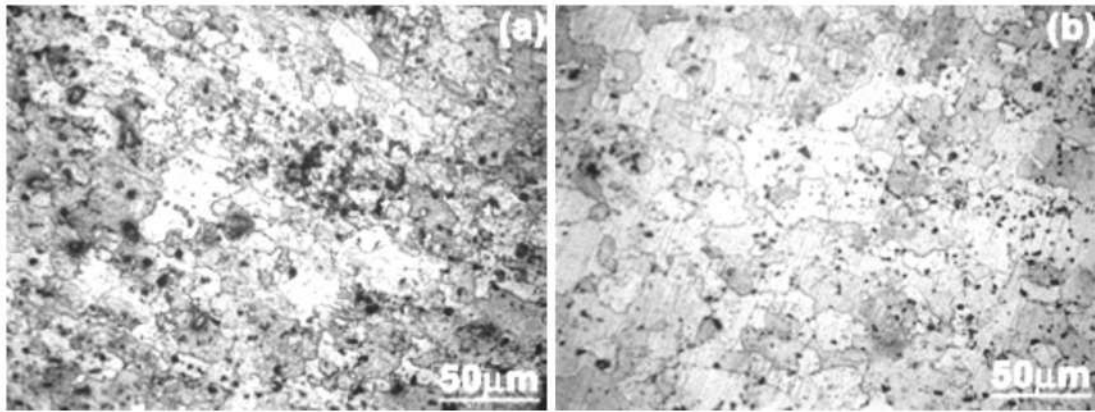
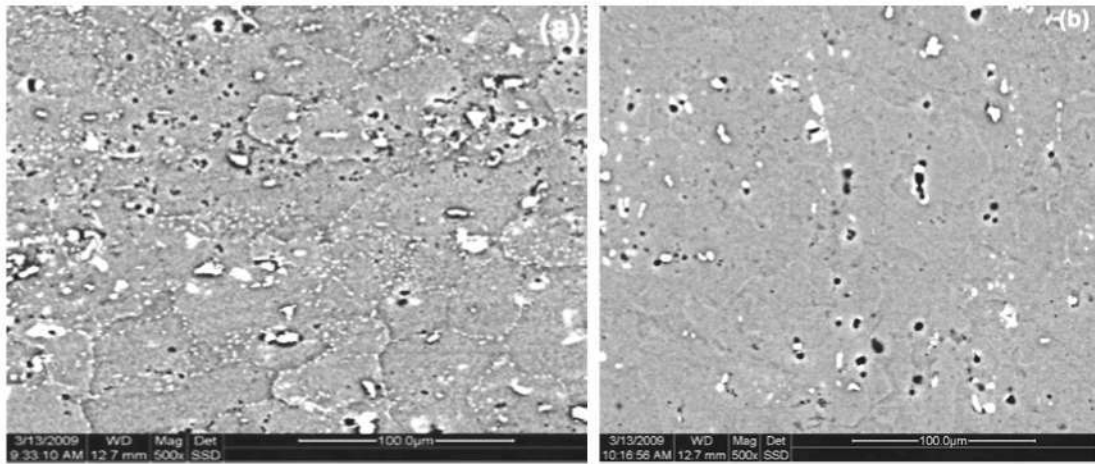Fig. 1 : Optical micrographs of base metal AA2014 (a) O condition (b) T4 condition

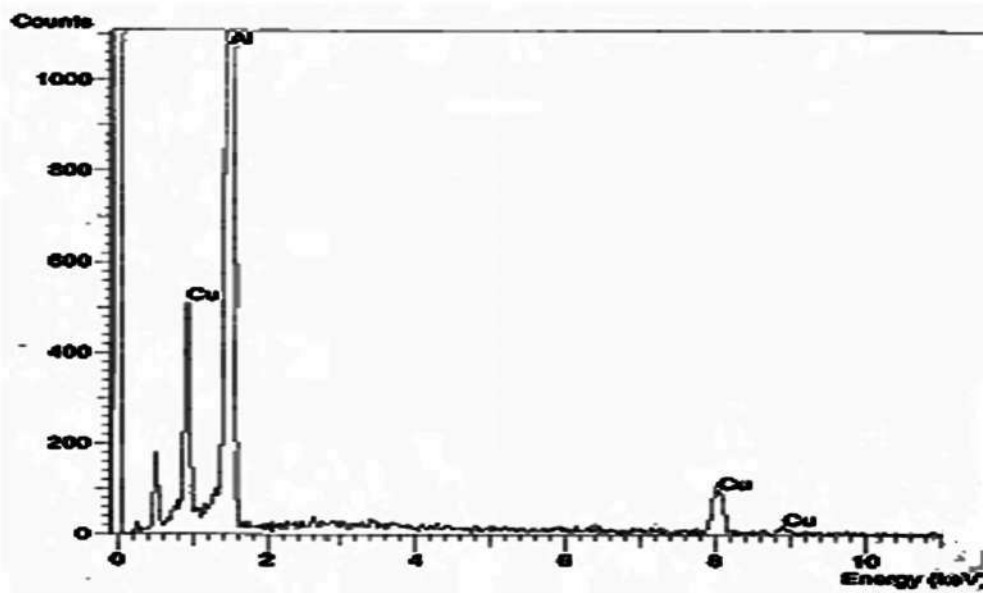Fig. 2 : SEM micrographs of base metal AA2014 (a) O condition (b) T4 condition

Fig. 3 : EDX spectrum of AA2014-T4 particle

31

Energy dispersive X-ray analysis (EDX) values of some randomly chosen particles indicated that Al/Cu weight ratios of these particles was close to that of about $53/47$ for è (Al_2Cu). The typical EDX spectrum of the particle is shown in **Fig. 3**. As an approximation, these particles will be considered as the è phase even though they may contain very small amounts of other elements as well. Several small particles within the grains and along the grain boundaries (GBs) were believed to be è phase, as they were too small to be analyzed by SEM-EDX.

The eutectic liquid during the terminal stage of solidification in
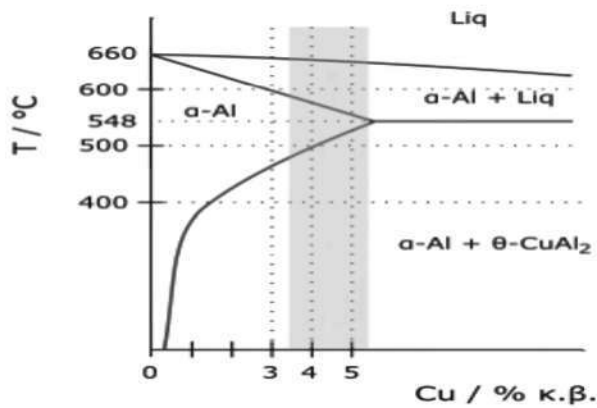
Fig. 4 : Al-Cu phase diagram

ingot casting solidifies and forms large and small eutectic particles along the grain boundaries and within grains. The solution heat-treating temperature for AA2014 alloy is 540°C. From the phase diagram (**Fig. 4**) the base metal is expected to consist of á-matrix plus additional undissolved è ($CuAl_2$) particles [14].

3.1.2 Gas Tungsten Arc (GTA) and Friction Stir (FS) Welds

The microstructures of various zones i.e. fusion zone (FZ), partially melted zone (PMZ) and heat affected zone (HAZ) present in GTA weld in O condition are shown in **Fig. 5**. The microstructures of three regions formed viz. Nugget Zone (NZ), Thermomechanically Affected Zone (TMAZ) and Heat Affected Zone (HAZ) during friction stir welding of AA2014 in T4 condition are shown in **Fig. 6**. When compared with GTA welding, it is observed that friction stir welding has not produced as cast coarse microstructure and solute segregation in the weld because it is a solid state process [15].

Fusion Zone/Nugget Zone

Optical microscopy of the fusion zone of AA2014 GTA weld reveals the eutectics of $CuAl_2$ and Mg_2Si appearing in the dendritic matrix of α-solid solution (**Fig. 7a**). The eutectics are present within the α-dendrites. SEM micrograph of fusion zone
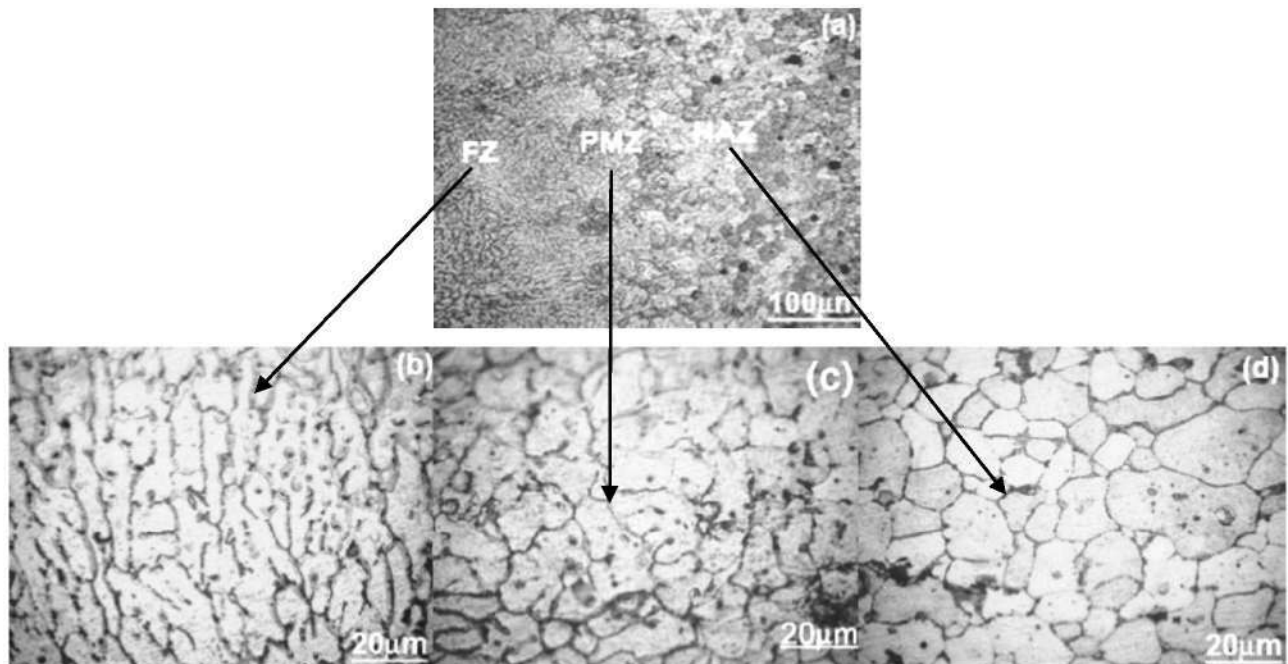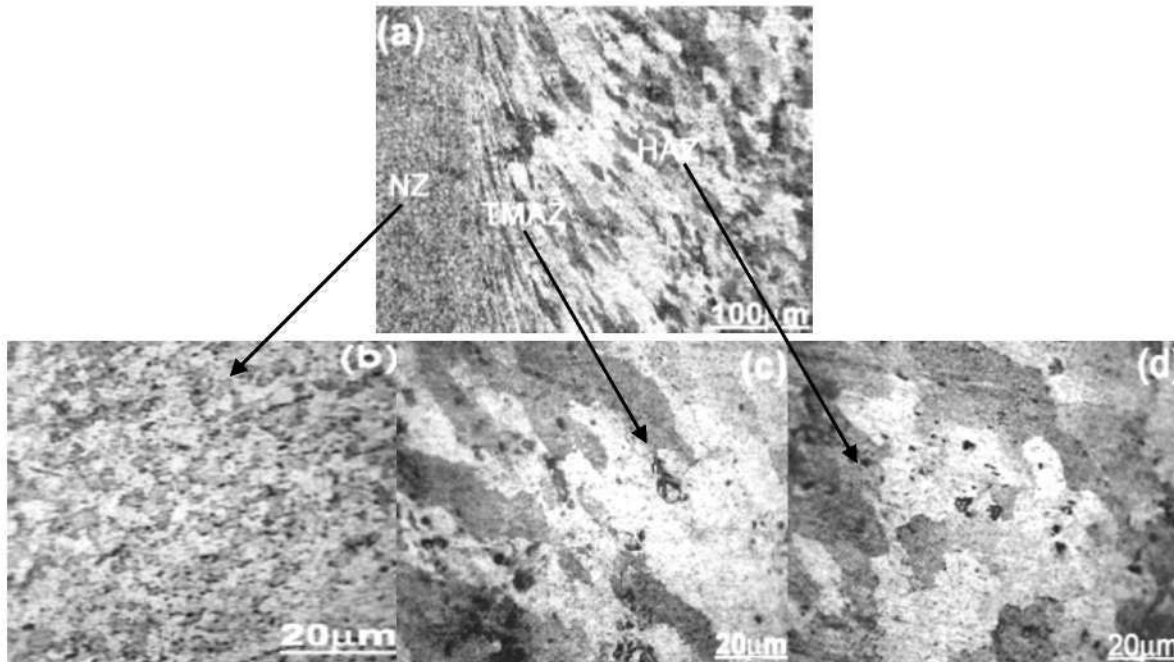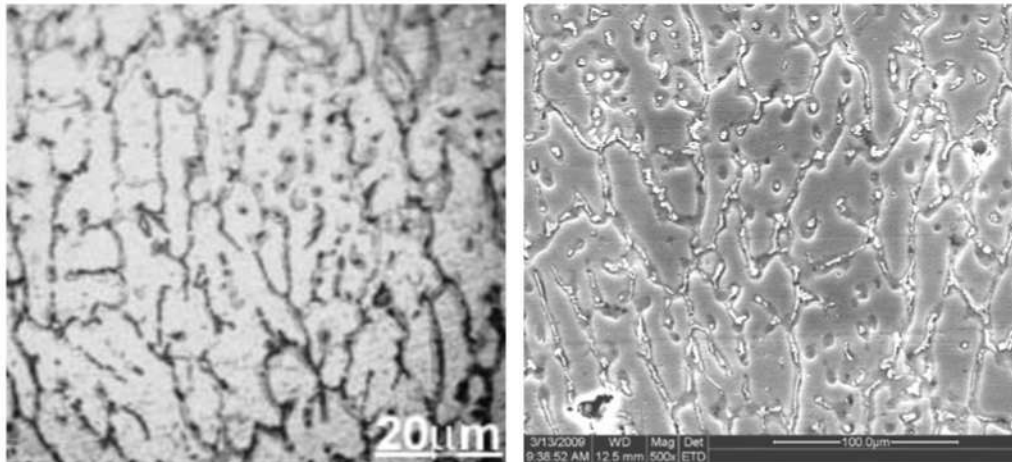
Fig. 5 : Optical microstructures of AA2014 GTA welds in O condition
(a) Formation of PMZ (b) FZ (c) PMZ   (d) HAZ

Fig. 6 : Optical microstructures of AA2014 FS welds in T4 condition
(a) Formation of NZ (b) NZ (c) TMAZ (d) HAZ

Fig. 7 : Optical and SEM micrographs of FZ in AA2014 GTA welds a) Optical b) SEM

of the weld is shown in **Fig. 7b**. Large columnar dendrites in the center and the epitaxial growth from the fusion line were observed in the fusion zone made by GTA welding process. The eutectics form as a thick and continuous net work in the fusion zones made by this welding process. Copper segregation to dendritic boundaries was more predominant in the fusion zones made by continuous current GTA welding. SEM studies revealed that coarse eutectic network present is continuous in the fusion zone of GTA weld.

Optical microstructures of NZ of AA2014 friction stir welds in O and T4 conditions are shown in **Fig. 8**. The nugget zone has fine globular eutectics in the order of 4-5 microns. Eutectics are randomly oriented. This indicated that, during the process of FSW, the copper rich eutectics have disintegrated into finer globular eutectics. The coarse dendrites and copper rich eutectics in the base metal are not present in the weld nugget. The redistribution of the eutectics indicated that the temperature obtained during the process is above the

solutionizing temperature but below the melting temperature of the alloy. The eutectics are comparatively fine and uniformly distributed in T4 condition (**Fig. 8b**) than that of O condition (**Fig. 8a**).

Partially Melted Zone / Thermomechanically Affected Zone

Aluminium-rich portion of the Al-Cu phase diagram is shown in **Fig. 4**. The big gap between the solidus and liquidus lines indicates that the Cu content of á phase (Al-rich solid) is much lower than that of the liquid. Since the percentage of copper content is about 15 times higher than the content of any other alloying element, alloy AA2014 can be considered as a binary alloy of Al-4.5% Cu as an approximation. It is observed from the optical micrographs of PMZ in AA2014 GTA welds in O and T4 conditions (**Fig. 9**) that the grain boundaries are darkly etched. According to the Al-Cu phase diagram, the liquation

zone is in the narrow region immediately outside the fusion zone, where the maximum temperature experienced during welding ranges from the liquidus temperature of about 642^0C on the fusion zone side to the eutectic temperature of 548^0C on the base metal side.

SEM micrographs of the PMZ of the AA2014 GTA welds in O and T4 conditions are shown in the **Fig. 10**. It can be observed that the coarsened á-aluminium dendrites with eutectic filled interdendritic regions occurred adjacent to the fusion zone. Coarsening of á-aluminium dendrites indicated partial melting of AA2014 GTA welds. This suggests that in PMZ the large á particles react eutectically with the surrounding á-matrix to become liquid and form large eutectic particles upon solidification. It is also noticed that the coarse and continuous eutectic network is observed in T4 condition (**Fig. 10b**) which may be attributed to more number of precipitates present in base metal in T4 condition.
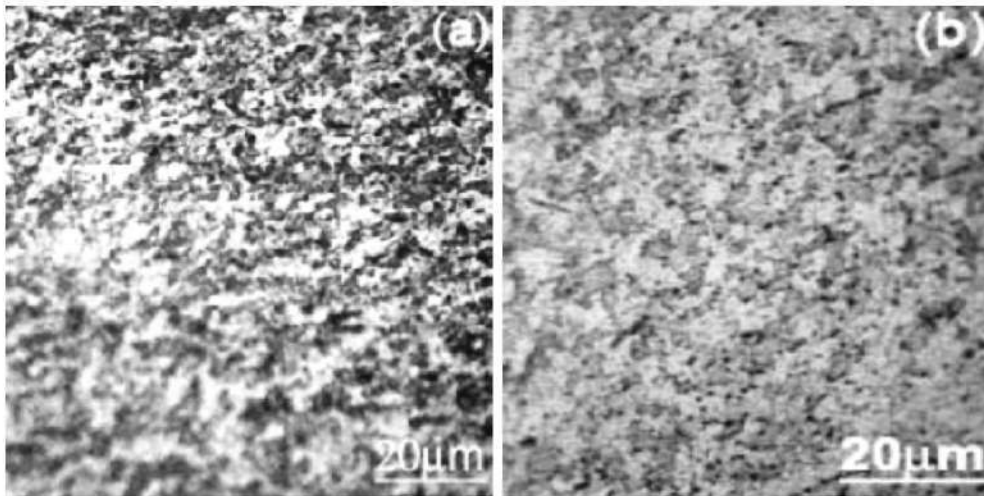

Fig. 8 : Optical micrographs of NZ in AA2014 FS welds
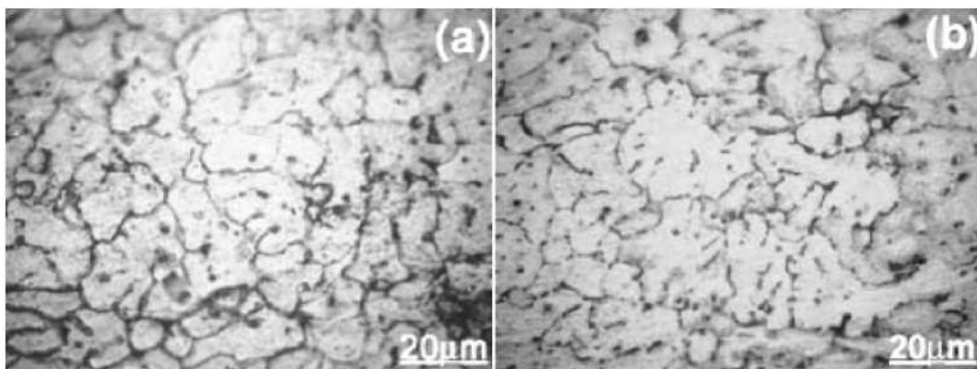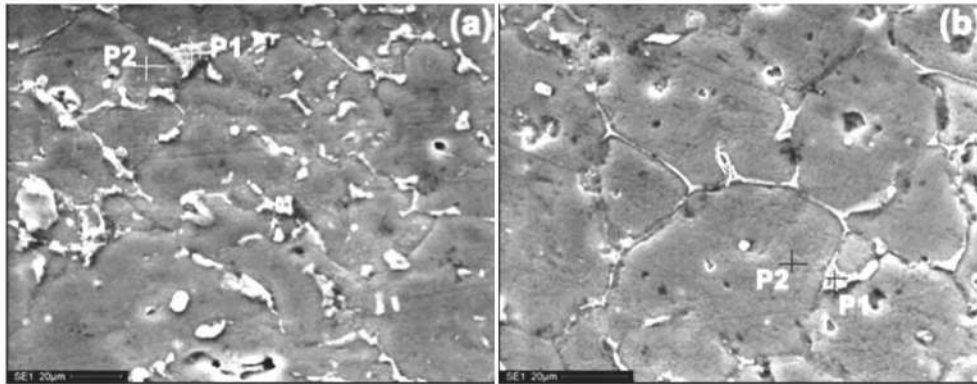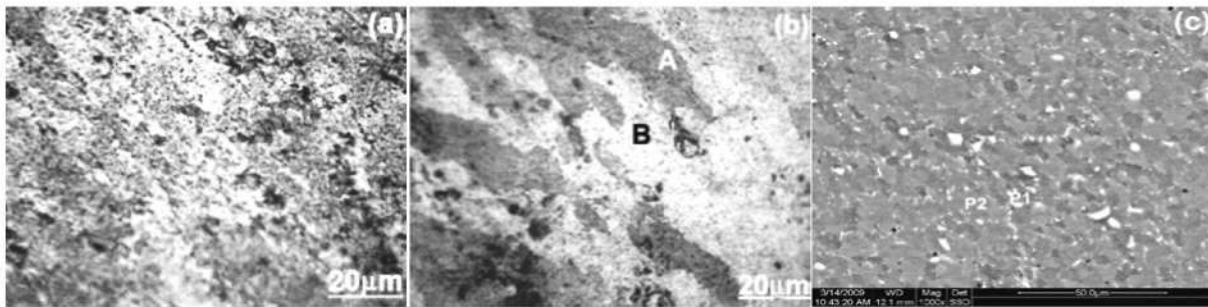**(a) O condition   (b) T4 condition**

Fig. 9 : Optical micrographs of PMZ in AA2014 GTA welds
(a) O condition   (b) T4 condition

Fig. 10 : SEM micrographs of PMZ in AA2014 GTA welds
O condition (b) T4 condition

Fig. 11 : Optical and SEM micrographs of TMAZ in AA2014 friction stir welds
(a) Optical of O condition(b) Optical of T4 condition (c) SEM of O condition

Thermomechanically affected zone is the transition zone between the base metal and weld nugget, characterized by a highly deformed structure in FS welds. The formation of thermomechanically affected zone in AA2014 friction stir welds is shown in **Fig. 6**. Optical micrographs of TMAZ in AA2014 friction stir welds in O and T4 conditions and SEM micrograph in O condition are shown in **Fig. 11**. The optical microstructures have shown a banded structure in both O and T4 conditions. It can be observed that the microstructure exhibited two discernable bands and the bands are arbitrarily labeled as A and B, with band A being the dark etching band (**Fig. 11(b)**). There is no significant change in the size and

morphology of coarser dendrites and eutectics, but their orientation is different in TMAZ from that of base metal. The eutectics are quite random. It is characterized as having elongated and newly formed grain structure.

SEM – EDX values at two selected points i.e. one at grain boundary (P1) and other in the matrix (P2) in PMZ of AA2014 GTA weld in O and T4 conditions are given in **Table 4**. The EDX values clearly indicated that the silicon enrichment at grain boundary is more than the copper enrichment. Filler metal used in GTA welding (AA4043) is the source of silicon enrichment. Precipitation of silicon at the grain boundaries of PMZ is more in T4 condition than that of O condition.

Table 4 : Composition (in Wt. %) of particles in PMZ (SEM-EDX)
in AA2014 GTA welds in O and T4 conditions

(a) O condition					(b) T4 condition			
Position	Mg	Al	Si	Cu	Position	Mg	Al	Si	Cu
P1 (GB)	01.07	80.64	14.82	03.48	P1 (GB)	00.61	64.55	32.96	01.88
P2 (Matrix)	01.43	93.35	02.68	02.54	P2 (Matrix)	01.50	96.20	00.83	01.46

Other source of liquation could be due to the remelting and resolidification of prior eutectics present in the base metal. Hot cracking in the partially melted zone was reported in many high strength aluminium alloys [16]. Huang and Kou [17] studied PMZ liquation in the gas metal arc welds of aluminum alloys and found that five different mechanisms can be used to describe the liquation. The formation of PMZ in AA2014 alloy can be explained from the portion of Al-Cu phase diagram shown in the **Fig. 12**.

SEM-EDX values taken at two different points i.e. one on the eutectic (P1) and the other in the matrix (P2) of TMAZ of AA2014 friction stir welds in O condition (**Fig. 11(c)**) are given in **Table 5**. Copper rich eutectics (CuAl$_2$) are predominant at grain boundary location. Where as in matrix copper percentages reported are very low. These eutectics are comparatively coarse in O condition than that of T4 condition.

3.2   Hardness studies

The hardness values of AA2014 GTA and FS welds in O and T4

Table 5: Composition (in Wt.%) of particles in TMAZ (SEM-EDX) of AA2014 friction stir welds in O condition

Position	Mg	Al	Cu
P1 (GB)	1.8	72.57	24.15
P2 (Matrix)	1.73	91.9	5.29

conditions are given in **Table 6**. Slightly higher hardness values are recorded in T4 condition than that of O condition in GTA welds. The hardness values obtained are in agreement with the SEM-EDX values observed. In FS welds, the hardness values indicate that the hardness is higher in O condition than that of T4 condition in NZ and TMAZ. These results are in agreement with the observed microstructures. The drop in hardness at TMAZ is due to the coarse-bent recovered grains.

It is also observed that the higher hardness values were recorded when the base metal is welded by friction stir welding process compared to that of GTA welding.

3.3   Pitting corrosion studies

Since PMZ width was very small, it was found difficult to test PMZ exclusively for corrosion. Hence pitting corrosion testing was done in the 1cm^2 exactly adjacent to fusion line and included both PMZ/TMAZ and HAZ. The pitting potential values of AA2014 GTA, FS welds and base metal in O and T4 conditions are given in **Table 7**. The values indicated that the pitting corrosion resistance of the FZ, PMZ/HAZ in T4 condition is better than that of O condition in GTA welding. This is attributed to coarsened eutectic network present in T4 condition than that of O condition. The values (**Table 7**) in FS welds indicated that the pitting corrosion resistance of the nugget zone and TMAZ/HAZ in T4 condition is better than that of O condition. The pitting corrosion results are in agreement with the observed copper enrichment at the grain boundary of
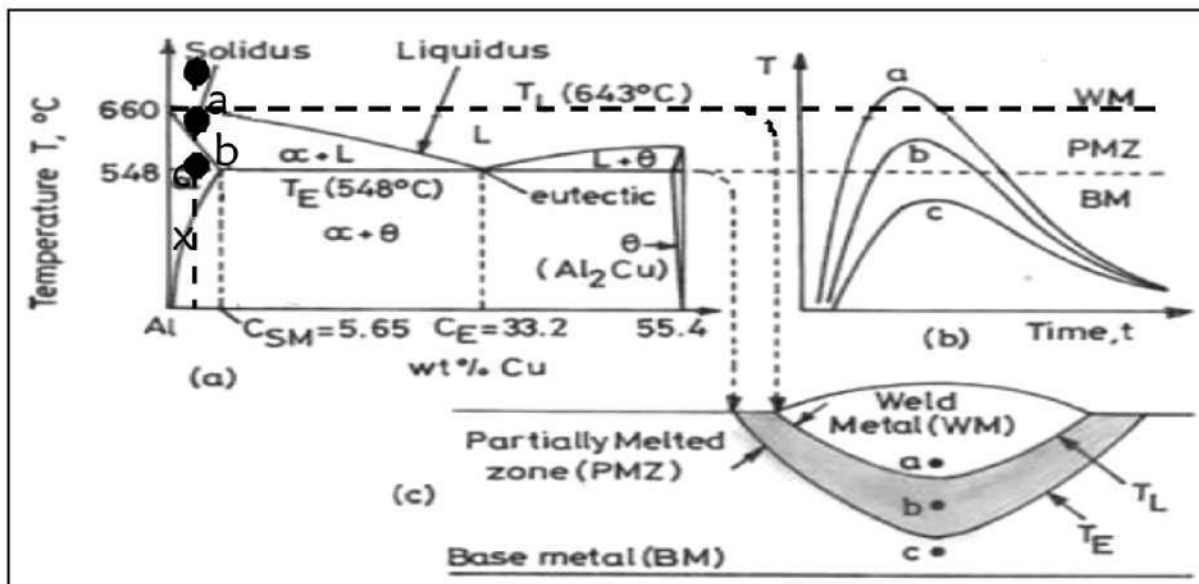

Fig. 12 : Formation of PMZ in AA2014 alloy welds

Table 6 : Vickers hardness values of AA2014 GTA and FS welds in O and T4 conditions

GTA Welds				Friction Stir Welds			
Condition	FZ	PMZ	HAZ	Condition	NZ	TMAZ	HAZ
O	62-66	97-105	81-93	O	126	105-110	111-115
T4	61-65	103-115	83-98	T4	112	102-106	112-120

**Table 7 : Pitting potentials, Epit (mV), SCE of AA2014 GTA and
FS welds and base metal AA2014 in O and T4 conditions**

GTA Welds and base metal				Friction Stir Welds		
Condition	FZ	PMZ/HAZ	BM	Condition	NZ	TMAZ / HAZ
O	-645	-672	-633	O	-592	-662
T4	-641	-659	-600	T4	-561	-589
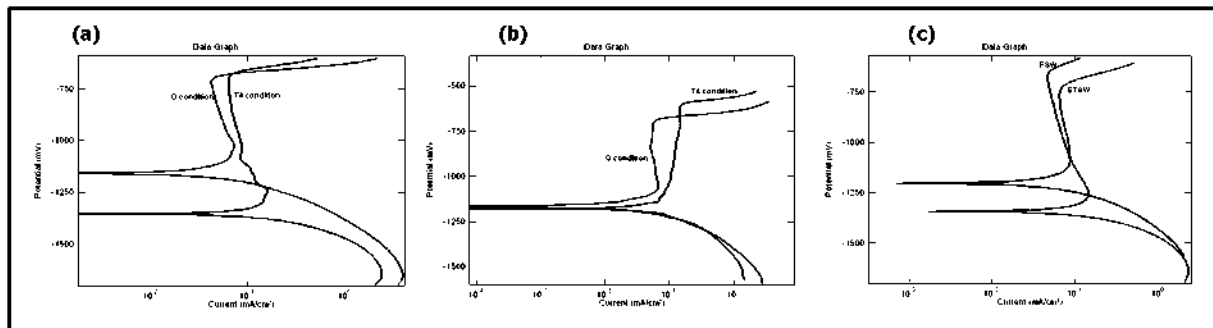
**Fig. 13 : Potentiodynamic polarization curves of AA2014 GTA and FS welds
(a) PMZ of GTA welds in O and T4 conditions (b) TMAZ of FS welds in O and T4 conditions
(c) FZ/NZ of GTA and FS welds in T4 condition**

the alloy in O condition. It is also observed that the pitting potential values (**Table 7**) in all the zones of friction stir welds are higher than that in GTA welds.

The critical potentiodynamic polarization curves in PMZ/TMAZ of the GTA and FS welds in O and T4 conditions are shown in **Fig. 13a & Fig. 13b** respectively. The curves also confirmed that the pitting corrosion resistance of the welds in PMZ/TMAZ is better in T4 condition than that of O condition. Poor corrosion of fusion zone and PMZ/HAZ of welds compared to that of base metal may be attributed to possible copper segregation. It is also confirmed from the curves (**Fig. 13c**) that the friction stir welds possess better corrosion resistance compared to that of GTA welds.

4.0   CONCLUSIONS

1. Fusion zone of AA2014 GTA welds exhibited coarser dendrites with continuous current GTA welding technique.

Eutectic net work was found to be continuous in the fusion zone of welds made with GTA welding. Copper segregation to grain boundaries was more predominant in the fusion zone of continuous current GTA weld.

2. Large copper rich eutectic particles were present within inter dendritic regions and were the clear indication of liquation in PMZ. This suggested that large Al$_2$Cu particles react eutectically with the surrounding α-matrix to become liquid and form large eutectic particles upon solidification. Other source of liquation could be due to the remelting and resolidification of prior eutectics present in the base metal.

3. Pitting resistance of PMZ/HAZ of AA2014 was found to be poor compared to base metal and fusion zone. This was attributed to the formation of copper rich dendrites at the grain boundary, which is highly cathodic to the region adjacent to the grain boundary. This resulted in the grooving of the surrounding matrix.

4. Microstructure in nugget zone has randomly oriented eutectics. This is attributed to disintegration of massive eutectics during friction stir welding and redistribution on subsequent cooling.

5. Potentiodynamic polarization tests of FS welded AA2014 alloy clearly indicated a greater pitting corrosion resistance of nugget zone than base metal. This is attributed to disintegration of eutectics present in the alloy. The higher pitting corrosion resistance of the nugget zone can be attributed to redistributed silicon rich eutectics.

6. The microstructure in TMAZ is characterized by a highly deformed structure. This is the transition zone between the base metal and nugget zone. Optical microstructures shown a banded structure.

7. TMAZ showed a poor pitting corrosion resistance when compared to base metal. During FS welding, this region heats up to a temperature just below the solutionizing temperature of the alloy. This results in coarsening of dendrites. The slightly more negative critical potentials of TMAZ can also be attributed to the residual stresses induced during FS welding.

8. Finally AA2014 FS welds have better hardness and corrosion properties than GTA welds.

REFERENCES

1. Huang. C and S. Kou. (2001); Partially melted zone in aluminium welds-solute segregation and mechanical behaviour, Welding Journal, 80, pp. 9s-17s.

2. Huang. C and S. Kou. (2001); Partially melted zone in aluminium welds-planar and cellular solidification, Welding Journal, 80, pp. 46s-53s.

3. Huang. C and S. Kou (2002); Liquation mechanisms in multi component aluminium alloys during welding. Welding Journal, 81; pp. 211s-222s.

4. Garland J.G. (1974); weld pool solidification control, British Welding journal, 22, pp.121-127.

5. Reddy G.M. (1997); Weld microstructure refinement in a 1441 grade Al-li alloy, J.Mater.Sci., 32, pp. 4117-4126.

6. Yamamoto, H., S. Harada, T. Ueyama, S. Ogawa, F. Matsuda and K. Nakata. (1993); Beneficial effects of low frequency pulsed MIG welding on grain refinement of weld metal and improvement of solidification cracking susceptibility of aluminium alloys, Welding International, 7(6), pp. 456-461.

7. Janaki Ram, G.D., G.M. Reddy and S. Sundaresan. (2000); Effect of pulsed welding current on the solidification structures in Al-Li-Cu and Al-Zn-Mg alloy welds, Practical Metallography, 37(5), pp. 276-288.

8. Rhodes, C. G., Mahoney, M. W., Bingel, W. H., Spurling, R. A., & Bampton, C. C. (1997); Effects of friction stir welding on microstructure of 7075 aluminum. Scripta Materialia : 36(1), pp. 69-75.

9. Dawes C.J., Thomas W.M.(1996); Friction stir process welds of aluminum alloys, Welding Journal, Vol.75, No.3, pp. 41-45.

10. Flores Valerio, O., Murr, L.E., McClure, J.C., et al. (1998); "Microstructural Issues in a Friction Stir Welded Aluminum Alloy", Scripta Materiala, Vol. 38, No. 5, pp. 703-708.

11. Murr, LE; Li, Y; Trillo, EA; Flores, RD; McClure, JC, (1998); Microstructures in friction-stir welded metals. Journal of Materials, Processing and Manufacturing Science, Vol. 7, pp. 145-161.

12. Liu, G., Murr, L.E., Niou, C-S., McClure, J.C., and Vega, F.R. (1997); "Microstructural Aspects of the Friction Stir Welding of 6061-T6 Aluminum", Scripta Materialia, Vol.37, No. 3, pp. 355-361.

13. Threadgill P.L (1999); Friction stir welding – the state of art, Bulletin 678; The welding Institute; Abington, Cambs; UK.

14. Polmear I.J (1997); Wrought aluminium alloys, Materials Science forum, pp. 21; 1-26.

15. W.M. Thomas, E.D. Nicholas, J.C. Needham, M.G. Nurch, P. Templesmith, C.J. Dawes (1995); Friction Stir Butt Welding. Int Patent App PCT/GB92/02203 and GB Patent App 9125978.8, December 1991, US Patent No. 5,460,317.

16. Dudas J.H. and F.R. Collins (1966); Preventing weld cracks in high-strength aluminium alloys. Welding Journal., 45; pp. 241s-249s.

17. Huang. C and S. Kou.(2000); Partially melted zone in aluminium welds-liquation mechanism and directional solidification, Welding Journal, 79; pp. 113s-120s.